

# Local adaptation in shell shape traits of a brooding chiton with strong population genomic differentiation

Priscila M. Salloum, PhD<sup>1,2</sup> , Shane D. Lavery, PhD<sup>1,3</sup>, Pierre de Villemereuil, PhD<sup>4</sup>, Anna W. Santure, PhD<sup>1</sup>

<sup>1</sup>School of Biological Sciences, University of Auckland, Auckland, New Zealand

<sup>2</sup>Department of Zoology, University of Otago, Dunedin, New Zealand

<sup>3</sup>Institute of Marine Science, Leigh Marine Laboratory, University of Auckland, Warkworth, New Zealand

<sup>4</sup>Institut de Systématique, Évolution, Biodiversité (ISYEB), École Pratique des Hautes Études | PSL, MNHN, CNRS, Sorbonne Université, Université des Antilles, Paris, France

Corresponding author: School of Biological Sciences, University of Auckland, Thomas Building, 3a Symonds Street, Auckland 1010, New Zealand. Email: [psal591@aucklanduni.ac.nz](mailto:psal591@aucklanduni.ac.nz)

## Abstract

Comparing divergence in quantitative traits and neutral molecular markers, such as  $Q_{ST}$ – $F_{ST}$  comparisons, provides a means to distinguish between natural selection and genetic drift as causes of population differentiation in complex polygenic traits. *Onithochiton neglectus* (Rochebrune, 1881) is a morphologically variable chiton endemic to New Zealand, with populations distributed over a broad latitudinal environmental gradient. In this species, the morphological variants cluster into 2 geographically separated shell shape groups, and the phenotypic variation in shell shape has been hypothesized to be adaptive. Here, we assessed this hypothesis by comparing neutral genomic differentiation between populations ( $F_{ST}$ ) with an index of phenotypic differentiation ( $P_{ST}$ ). We used 7,562 putatively neutral single-nucleotide polymorphisms (SNPs) across 15 populations and 3 clades of *O. neglectus* throughout New Zealand to infer  $F_{ST}$ .  $P_{ST}$  was calculated from 18 shell shape traits and gave highly variable estimates across populations, clades, and shape groups. By systematically comparing  $P_{ST}$  with  $F_{ST}$ , we identified evidence of local adaptation in a number of the *O. neglectus* shell shape traits. This supports the hypothesis that shell shape could be an adaptive trait, potentially correlated with the ability to live and raft in kelp holdfasts.

**Keywords:** local adaptation, *Onithochiton neglectus*,  $P_{ST}$ – $F_{ST}$  comparisons, shell shape

Comparing populations across heterogeneous environments provides a means to investigate the mechanisms underlying phenotypic divergence (Blanquart et al., 2013; Kawecki & Ebert, 2004). Observed phenotypic variation among populations may be neutral or adaptive, and adaptive phenotypic variation can result from evolutionary changes (local adaptation) or adaptive phenotypic plasticity (Grenier et al., 2016; Kawecki & Ebert, 2004; Sanford & Kelly, 2011).

In order to study adaptive phenomena, common garden experiments have frequently been used to minimize the environmental variance within controlled conditions (de Villemereuil et al., 2016; Kawecki & Ebert, 2004). Coupling common garden experiments with controlled backcrosses or known genealogies, it is possible to infer an index of between-population differentiation in quantitative traits ( $Q_{ST}$ ), which accounts for the additive genetic variance within and between populations (Ab-Ghani et al., 2012; de Villemereuil et al., 2016; Spitze, 1993). Following the estimation of  $Q_{ST}$  and to assess the relative roles of natural selection and genetic drift in inter-population divergence, a null hypothesis of neutral evolution can be tested by estimating genetic differentiation at neutral markers ( $F_{ST}$ ), and then comparing it to  $Q_{ST}$  (Spitze, 1993). In general, it is expected that  $Q_{ST}$  will be equal to  $F_{ST}$  if drift is the sole evolutionary

force acting on the differentiation of the traits for which  $Q_{ST}$  is estimated (Spitze, 1993, but see de Villemereuil et al., 2020, Miller et al., 2008; Santure & Wang, 2009). If  $Q_{ST}$  is significantly larger than  $F_{ST}$ , divergent selection is likely to be acting, whereas if  $Q_{ST}$  is significantly smaller than  $F_{ST}$ , stabilizing selection is likely (Leinonen et al., 2013; Merilä, 1997; Merilä & Crnokrak, 2001; Spitze, 1993).

However, when dealing with species for which artificial rearing is challenging, common garden experiments are unattainable, and therefore  $Q_{ST}$  cannot be directly estimated (Leinonen et al., 2013). As an alternative, the literature has advocated the use of its proxy,  $P_{ST}$ , which is estimated using phenotypic data measured directly from wild populations (Brommer, 2011; Leinonen et al., 2013). In this case, although information is lacking on the proportion of additive genetic effects describing variation within populations ( $h^2$ ) and across populations ( $c$ ), a hypothesis (usually  $c = h^2$ ) can be used to estimate  $P_{ST}$  (Leinonen et al., 2013; Pujol et al., 2008; Whitlock & Gilbert, 2012). To assess the robustness of  $P_{ST}$  as a proxy for  $Q_{ST}$ , comparisons of  $F_{ST}$  and  $P_{ST}$  are then made for a range of hypothetical  $c$  and  $h^2$  values (Brommer, 2011). In the wild, environmental differences between populations might be large, thus  $c$  might be much smaller than  $h^2$  (Brommer et al., 2014). In a scenario where  $P_{ST} > F_{ST}$  even

Received November 5, 2021; revisions received September 13, 2022; accepted November 24, 2022

© The Author(s) 2022. Published by Oxford University Press on behalf of The Society for the Study of Evolution (SSE).

This is an Open Access article distributed under the terms of the Creative Commons Attribution License (<https://creativecommons.org/licenses/by/4.0/>), which permits unrestricted reuse, distribution, and reproduction in any medium, provided the original work is properly cited.

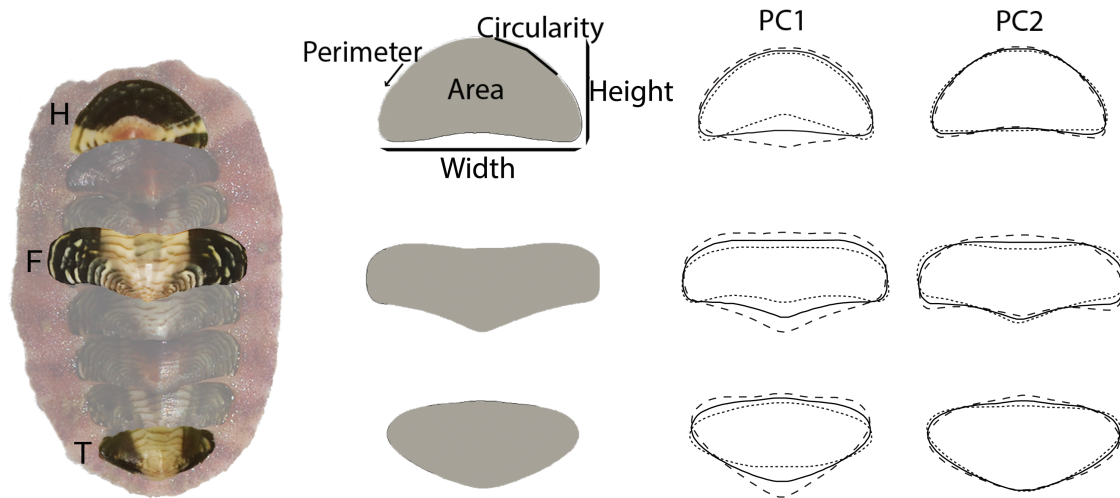


**Figure 1.** Schematic representation of the traits measured in three of the valves of each chiton. H: head valve; F: fourth valve; T: tail valve. The raw measurements (area, perimeter, circularity, length, and width) were measured in all three valves but are only represented in the head valve for clarity. PC1 and PC2 contours represent the mean (solid outline)  $\pm$  standard deviation (dotted lines) of variation in the shape of each of the valves for all individuals, corresponding to the graphical output of the geometric morphometrics analyses undertaken in Salloum et al. (2020), using the software SHAPE v.1.3 (Iwata & Ukai, 2002).

when  $c$  is small compared to  $b^2$ , phenotypic differentiation is likely larger than expected if only between-population environmental effects were considered, and thus  $P_{ST}$  is treated as a reliable  $Q_{ST}$  proxy (Brommer et al., 2014). The opposite is true when  $P_{ST}$  is below the expected differentiation ( $P_{ST} < F_{ST}$  for a large  $c$ ) (Brommer et al., 2014). Thus, if  $P_{ST} \gg F_{ST}$  and  $cb^2 \ll 1$ , local adaptation is possibly inflating phenotypic differentiation between populations; if  $P_{ST} \ll F_{ST}$  and  $cb^2 \gg 1$ , phenotypic differentiation between populations might be restricted by stabilizing selection consistent across populations (Brommer, 2011).

Here, we used  $P_{ST}$ - $F_{ST}$  comparisons to assess the relative roles of neutral and adaptive forces in shell shape divergences observed in a chiton endemic to New Zealand, *Onithochiton neglectus* Rochebrune, 1881. Molluscs have an astounding diversity in shell shapes, but chitons have a rather conserved shell morphology, which has remained similar to its Palaeozoic ancestral form throughout geological time (Sigwart, 2009; Sigwart et al., 2013, 2015; Sirenko, 2006). The use of shell morphology has, therefore, posed challenges for chiton taxonomy (Sigwart et al., 2013; Sirenko, 2006), and the link between chiton shell shape and adaptive evolution has been little explored. Resolving the relationship of chitons with other molluscs is key to help determine the confusing phylogenetic relationship among all other molluscs (generally, chitons are placed closer to the outgroup) (Sigwart & Lindberg, 2015). Therefore, understanding evolution of their constrained shell shape is important to help contextualize shell diversification in the whole phylum (Sigwart et al., 2013). *O. neglectus* is a clear example in which local adaptations is likely, due to its phenotypically variable populations distributed over a wide latitudinal range, and low connectivity among populations due to a brooding development mode (Salloum et al., 2020, 2022). Furthermore, *O. neglectus* habitats in the south are commonly dominated by bull kelp *Durvillaea* species, but bull kelp is relatively rare in the north of the distribution (Naylor, 1951). This means that North Island *O. neglectus* are rarely found in the holdfasts of this algae,

while the southern populations are known to hitchhike over long distances in the holdfasts of this highly buoyant kelp (Creese, 1988; Morton & Miller, 1973; Nikula et al., 2012; Spalding et al., 2012; Waters et al., 2018). Previous work has demonstrated three well-supported clades of *O. neglectus* (North, Central, and South) with no connectivity among them (Salloum et al., 2020, 2022). The three clades appear to have diverged from each other at approximately the same time, around 10 Mya ago (Salloum et al., 2020).

Genetic and morphological differences between northern and southern populations (corresponding to North + Central, and South genetic clades, respectively) of *O. neglectus* have been detected, and shell shape has been hypothesized to be an adaptive trait correlated with *Durvillaea* species association (Salloum et al., 2020). Here, we investigated this hypothesis by (a) assessing the distribution of neutral genetic variation across New Zealand populations of *O. neglectus* in order to infer the level of phenotypic differentiation that would be expected due to genetic drift alone and (b) measuring the phenotypic differentiation of quantitative measures of shell shape across these populations in order to perform  $P_{ST}$ - $F_{ST}$  comparisons for a range of  $c$  and  $b^2$ , assessing the likelihood of adaptation in shell shape.

We assessed 15 populations of *O. neglectus* with 7,562 putatively neutral single-nucleotide polymorphisms (SNPs). Neutral  $F_{ST}$  was estimated between all populations and compared with  $P_{ST}$  estimated from shell shape traits (raw quantitative measurements of head, tail, and fourth valve perimeter, circularity, height, and width, and also geometric morphometrics [shape] of these valves, Figure 1). This approach enabled us to quantify the phenotypic differentiation in shell traits across populations and identify phenotypic differentiation in the shell shape that deviates from the expected differentiation based on neutral genetic markers. We expected that most shell traits would conform to neutrality, due to high variability in shell shape within populations (Salloum et al., 2020), but that differentiation in some traits would be larger than expected (particularly that between northern and southern populations) and potentially adaptive.

**Methods**

**Genomic data**

The samples used here have featured in previous studies describing geometric morphometrics of shell shape and population genetic analyses (Nikula et al., 2012; Salloum et al., 2020, 2022). Individuals come from 16 populations of *O. neglectus* distributed across New Zealand and its

Sub-Antarctic Islands (with one population subsequently removed during analysis), comprising the previously identified two shape groups and three genetic clades (Figure 2E,F; Salloum et al., 2020, 2022). Between 5 and 20 individuals were sampled per population. DNA extraction and initial checks of concentration and purity were undertaken following the protocol described in Salloum et al. (2020). In brief,

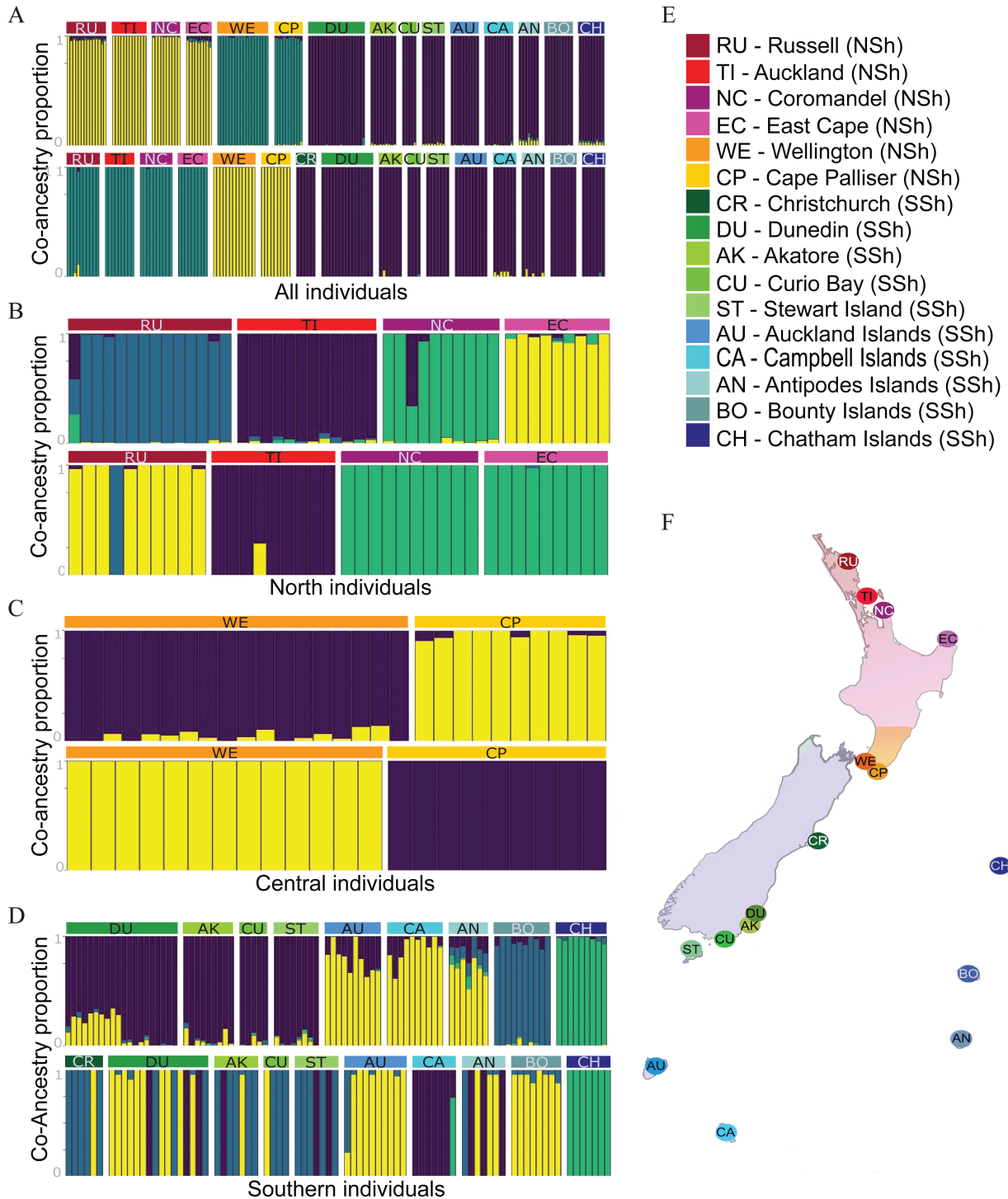


**Figure 2.** Co-ancestry matrices comparing genomic SNP (top) and mtDNA COI (bottom). Each bar represents one individual, and colors represent different ancestral populations (K). (A) All populations, for K = 3; (B) populations of the North clade, for K = 4; (C) populations of the Central clade, for K = 2; (D) populations of the South clade, for K = 4; (E) Population key, with abbreviations and shape groups (NSh is northern shape group; SSh is southern shape group); (F) Map of sampling locations, color-coded and indicating the three genetic clades.

samples with high molecular weight DNA were selected for genotyping by sequencing, utilizing enzymes *Pst* I and *Msp* I and sequencing across two lanes on an Illumina HiSeq (169 samples and 19 replicates). Following demultiplexing and quality control, SNPs were called with Stacks v 2.4 (Catchen et al., 2011, 2013) using a population map specifying all 16 populations and the following parameters:  $m = 3$ ,  $M = 2$ ,  $n = 4$ ,  $r = 0.8$ , a minor allele frequency filter of 0.05, and one random SNP per locus to avoid strong linkage disequilibrium (Supplementary Material, AMD1; Supplementary Figures S1 and S2). Pairwise Hamming genetic distances of populations and technical replicates were calculated using the R package Poppr v. 2.9.1 (Kamvar et al., 2014, 2015; Supplementary Figure S3). Subsequent analyses were carried out using a dataset containing no replicates (169 individuals), which were selected by choosing the replicated sample with the larger number of SNPs from the previous run. Further filtering consisted of removing individuals with more than 90% missing data (two individuals) using the SNP\_GBS filter pipeline (Alexander, 2018) and loci with more than 30% missing data using VCFtools v. 0.1.14 (Danecek et al., 2011). This completely removed one population (Christchurch—CR) from the dataset (Supplementary Figure S4).

To focus the analyses on putatively neutral loci, the resulting dataset containing 9,275 SNPs, 161 individuals, and 15 populations was analyzed with BayeScan (Foll & Gaggiotti, 2008), using default configurations. Based on a differentiation coefficient ( $F_{ST}$ ) and a false discovery rate of 0.05, 1,713 loci were flagged as outliers and were conservatively removed from the dataset. Given the high level of population structure and differentiation across the three *O. neglectus* clades (Salloum et al., 2020, 2022), this approach is likely to have excluded a number of neutral loci along with putatively adaptive loci, and is unlikely to have removed all adaptive loci, but the aim was to enrich the proportion of neutral loci for subsequent analyses. The resulting putatively neutral dataset contained 7,562 SNPs.

Population mean sequencing depth across sites was calculated by taking the average sequencing depth of all sites for each individual and then averaging it for the population, using --site-depth in VCFtools v. 0.1.14 (Danecek et al., 2011). Similarly, --het in VCFtools was used to calculate population mean expected and observed homozygosity, which counted expected and observed homozygous sites for each individual and divided it by the total number of genotyped sites per individual, then averaged per population. Population expected heterozygosity was calculated with Adegnet v. 2.1.1 (Jombart, 2008; Jombart & Ahmed, 2011). Population mean observed heterozygosity and nucleotide diversity were calculated with the R package pegas v. 0.13 (Paradis, 2010).

### Genomic population differentiation

To confirm that SNP data recovered the same population structure as previously described from single-locus data, SNPs and mtDNA cytochrome c oxidase I (COI) were compared in co-ancestry matrices built with sparse nonnegative matrix factorization (snmf) implemented in the R package LEA v. 2.6.0 (Frichot & François, 2015), with the best number of populations chosen based on the cross-entropy criterion (Supplementary Figure S5).

Using the neutral SNPs, the hierarchical partitioning of genetic variation was investigated with analyses of molecular variance (AMOVAs), performed in GeneAEx v. 6.51

(Peakall & Smouse, 2006, 2012), and the overall and pairwise  $F_{ST}$  (Wright's  $F_{ST}$ , calculated following Meirmans and Hedrick [2011]) were obtained, with 9,999 random permutations to test statistical significance. Different AMOVAs were performed for individuals partitioned across 15 populations, individuals partitioned across three clades (North, Central, and South), and individuals partitioned across the two previously identified northern and southern shell shape groups (Salloum et al., 2020). The northern shell shape was found in all populations belonging to the North and Central genetic clades, while the southern shell shape was found in all populations in the South genetic clade (Salloum et al., 2020). The significance of the population pairwise  $F_{ST}$  indices were corrected for multiple testing using the method of Benjamini and Yekutieli (2001). The pairwise  $F_{ST}$  indexes estimated with the neutral SNPs were directly compared with pairwise  $\Phi_{ST}$  results from the COI gene of previously undertaken analyses (Salloum et al., 2020).

### Phenotypic population differentiation

To estimate indices of phenotypic differentiation ( $P_{ST}$ ) for shell shape across populations, a dataset with quantitative traits was generated with raw measurements of size of the head, fourth and tail valves of the genotyped chitons (area, perimeter, circularity, height, and width of the valves), plus geometric morphometric analyses of closed contours of the same valves to capture overall shape (Figure 1). Most chitons have a shell composed of eight valves: a head valve, six intermediate valves (which are relatively similar in shape), and a tail valve. The traits measured here were chosen because they thoroughly describe the external shape of three distinctive valves per animal (the head, one of the intermediate valves, and the tail). In addition, these traits are amenable to the consistent measurement between fresh and preserved specimens, even without taking the valves apart from the body, which is important when working with rare samples from remote locations. Previous findings indicate that these traits could present adaptive variation between shell shape groups, as they differentiate *O. neglectus* populations along their north-south distribution (Salloum et al., 2020). The methods and results of the geometric morphometric analyses were reported elsewhere, with the first and second principal components of shape responsible for most of the variation in each of the head, fourth and tail valves (76.6%, 89.1%, and 69.6%, respectively; Salloum et al., 2020) and used in the subsequent analyses. The raw valve measurements were undertaken with Photoshop CC 2015, following the same protocol used to measure valve area in Salloum et al. (2020). The final phenotypic dataset contains six traits for each of the three valves, 101 individuals and 15 populations (all with SNP genotypes available). All traits were corrected to eliminate allometric size variation by using the residuals from a linear regression (Outomuro & Johansson, 2017), in which the area of the fourth valve was set as the explanatory variable. The distribution of these traits was then checked, ensuring these are continuous measurements and not discrete groups, and a principal component analysis (PCA) was carried out to visualize shell shape patterns in all traits and all individuals.

The R package Pstat v. 1.2 (Silva & Silva, 2018) was used to estimate the indices of phenotypic differentiation ( $P_{ST}$ ) of shell shape for individuals categorized in the same three ways used in the calculations of  $F_{ST}$  (15 populations, three genetic clades, and two shape groups).  $P_{ST}$  was calculated for the

three valves (fourth, head, and tail) for the following traits: perimeter, circularity, height, width, and the scores of the first two principal components of shape (PC1 and PC2).  $P_{ST}$  for each shell trait was initially calculated under the assumption that the proportions of phenotypic variation due to additive genetic effects between and within populations are equal ( $c = b^2$ ). Subsequently, a range of  $clb^2$  values were used for estimating  $P_{ST}$  under varying hypothetical scenarios of within- and between-population variation, which enabled the sensitivity of the outcomes of the  $P_{ST} - F_{ST}$  contrast to be tested (Brommer, 2011). Confidence intervals for the  $P_{ST}$  estimates were set using 1,000 bootstrap resamples, and comparisons were made between the  $P_{ST}$  estimates and the putatively neutral  $F_{ST}$  values estimated with the AMOVAs. Local adaptation is probable when  $P_{ST}$  and its upper and lower 95% confidence intervals are larger than  $F_{ST}$  for a critical  $clb^2 \leq 1$ , but it is strongly supported for a critical  $clb^2 \leq 0.5$  (Brommer, 2011). Finally, to check for a signal of increasing trait differentiation with increasing distance between populations, the correlation between a metric of  $P_{ST}$  of each trait ( $P_{ST}/(1-P_{ST})$ ) and geographical distance (log (distance in kilometers)) was tested with a Mantel test using the R package ade4 v. 1.7.19 (Dray & Dufour, 2007), with 9,999 permutations, and a Benjamini-Yekutieli correction for multiple testing (Benjamini & Yekutieli, 2001).

## Results

Our final dataset represents the three genetic clades, with the 15 population sample sizes varying from 5 to 20 individuals (Table 1). Across the 7,562 SNPs used in the analyses, the mean sequencing depth of all sites across populations ranged from 14.01 in the Antipodes Islands to 31.15 in Auckland (Table 1). Overall, populations have low heterozygosity and generally low nucleotide diversity in these loci (Table 1).

## Genomic patterns

The co-ancestry matrices strongly supported the existence of the three *O. neglectus* clades previously described, corresponding to North, Central, and South genetic clades, with the last including populations from the South Island, the Sub-Antarctic Islands, and Chatham Islands (Figure 2). The population structure determined using SNPs is largely concordant with that previously determined using COI (Figure 2A–D). The same three clades are consistently retrieved in phylogenetic trees of SNPs and COI (Supplementary Material, AMD2; Supplementary Figure S6) and were also observed in previous analyses of the 16S gene and the nuclear ITS (Salloum et al., 2020).

The  $F_{ST}$  values reflected the strong differentiation among populations (overall  $F_{ST} = 0.57$ ,  $p < .001$ ), with the South clade the most differentiated (Table 2). The population pairwise  $F_{ST}$  values were much higher for comparisons of populations between clades than within a clade (Figure 3A; Supplementary Table S1). After correcting for multiple tests, all pairwise  $F_{ST}$  indices estimated between populations from different clades remained significant, as well as many population comparisons within clades. Within the North clade, only Russell (RU,  $n = 14$ ) was significantly divergent from other sampled populations. In the Central clade, the single pairwise comparison (between Wellington [WE] and Cape Palliser [CP]) was not significant. Within the South clade, a number of pairwise comparisons were significant, with the Chatham Islands (CH), Bounty Islands (BO), and Antipodes Islands (AN) being the most divergent South populations. When compared to  $\Phi_{ST}$  previously estimated with COI (Salloum et al., 2020), the levels of differentiation are generally smaller and less significant for the SNPs, but the datasets show a similar pattern (Supplementary Figure S7).

**Table 1.** Summary of the final SNP dataset after filtering and removal of outlier loci identified with BayeScan.

Clade	Pop	Geno_Inds	Mean depth	Mean O_Hom	Mean E_Hom	Mean Nuc_div	Mean E_Het	Mean O_Het
North	RU	14	29.01	0.932	0.660	0.114	0.239	0.069
	TI	12	31.15	0.921	0.661	0.006	0.233	0.085
	NC	10	20.68	0.944	0.660	0.016	0.206	0.050
	EC	9	22.71	0.941	0.658	0.024	0.274	0.059
Central	WE	18	25.31	0.948	0.670	0.009	0.206	0.052
	CP	10	27.84	0.955	0.670	0.018	0.236	0.047
South	DU	20	22.03	0.988	0.667	0.011	0.211	0.013
	AK	9	24.06	0.993	0.667	0.007	0.077	0.007
	CU	5	21.59	0.995	0.667	0.019	0.026	0.006
	ST	8	19.11	0.993	0.668	0.162	0.080	0.007
	AU	10	17.99	0.991	0.667	0.011	0.032	0.011
	CA	10	18.13	0.991	0.667	0.010	0.039	0.010
	AN	7	14.01	0.989	0.669	0.007	0.150	0.012
	BO	10	19.63	0.983	0.667	0.009	0.044	0.018
CH	9	14.80	0.985	0.669	0.014	0.123	0.017	

*Note.* Pop = population; Geno Inds = number of individuals successfully genotyped per population; Mean depth = population-averaged mean depth of all sites in each individual; Mean O\_Hom = population-averaged observed homozygosity; Mean E\_Hom = population-averaged expected homozygosity; Mean Nuc\_div = population mean nucleotide diversity; Mean E\_Het = population mean expected heterozygosity; and Mean O\_Het = population mean observed heterozygosity. Population key: RU = Russell, TI = Auckland, NC = Coromandel, EC = East Cape, WE = Wellington, CP = Cape Palliser, DU = Dunedin, AK = Akatore, CU = Curio Bay, ST = Stewart Island, AU = Auckland Islands, CA = Campbell Island, AN = Antipodes Islands, BO = Bounty Islands, CH = Chatham Islands.

**Table 2.** Indices of neutral genetic differentiation ( $F_{ST}$ ), and phenotypic differentiation ( $P_{ST}$ ) in all analyzed traits, among the 15 sampled populations, three genetic clades, and two shape groups.

Index	Trait	15 Pops	3 genetic clades			2 shape groups
		Overall	NxC	NxS	CxS	NSh x SSh
$F_{ST}$	Neutral SNPs	0.57	0.48	0.69	0.72	0.49
$P_{ST}$ Fourth valve	Perimeter	0.73	0.51	0.88	0.31	0.80
	Circularity	<b>0.93</b> ‡	0.00	<b>0.94</b> ‡	<b>0.92</b>	<b>0.96</b> ‡
	Height	<b>0.91</b> ‡	0.47	<b>0.94</b> ‡	0.88	<b>0.95</b> ‡
	Width	<b>0.84</b>	0.87	<b>0.91</b>	0.26	<b>0.86</b>
	Shape PC1	<b>0.94</b> ‡	0.83	<b>0.96</b> ‡	<b>0.90</b>	<b>0.97</b> ‡
	Shape PC2	0.69	0.37	0.82	0.45	0.79
$P_{ST}$ Head valve	Perimeter	<b>0.85</b>	0.09	<b>0.88</b>	0.87	<b>0.92</b> ‡
	Circularity	0.81	0.19	0.87	0.75	<b>0.89</b> ‡
	Height	0.72	0.22	0.70	0.80	0.83
	Width	<b>0.91</b> ‡	0.27	<b>0.94</b> ‡	0.88	<b>0.95</b> ‡
	Shape PC1	<b>0.90</b> ‡	0.78	<b>0.95</b> ‡	0.64	<b>0.92</b> ‡
	Shape PC2	0.50	0.71	0.49	0.36	0.04
$P_{ST}$ Tail valve	Perimeter	0.61	0.54	0.77	0.03	0.63
	Circularity	0.73	0.26	0.70	0.80	0.84
	Height	<b>0.92</b> ‡	0.66	<b>0.95</b> ‡	<b>0.88</b>	<b>0.96</b> ‡
	Width	0.45	0.02	0.57	0.41	0.62
	Shape PC1	0.76	0.20	0.83	0.70	<b>0.86</b>
	Shape PC2	0.82	0.85	0.64	0.86	0.28

Note. Overall,  $F_{ST}$  and  $P_{ST}$  were estimated for the individuals partitioned into 15 populations (15 Pops); Pairwise estimates correspond to North versus Central clades (NxC), North versus South clades (NxS), Central versus South clades (CxS), and northern shape group versus southern shape group (NSh x SSh). **Bold-type** indicates comparisons for which  $P_{ST}$  and its upper and lower 95% confidence intervals were larger than  $F_{ST}$  for a critical  $cl/b^2 = < 1$ ; **bold-type** and ‡ indicates comparisons with critical  $cl/b^2$  value  $= < 0.5$  (stronger support for local adaptation). All  $F_{ST}$  values had  $p < .001$ .

### Phenotypic patterns

The shell traits measured show continuous variation (Supplementary Figure S8), and the previously reported pattern of North + Central versus South shell shapes is clearly confirmed in the PCA (Supplementary Figure S9). The  $P_{ST}$  estimates were highly variable, reflecting very strong phenotypic differentiation among populations in some traits of each valve, but little to no differentiation in others (Table 2). There is no correlation between geographical distance and the  $P_{ST}$  of any trait (Supplementary Table S2). The highest  $P_{ST}$  of 0.97 was estimated from the PC1 of the fourth valve, comparing northern and southern shape groups, and the minimum  $P_{ST}$  of 0.00 was estimated from the circularity of the fourth valve, comparing North and Central clades. As expected, the  $P_{ST}$  of the first principal component score (PC1) is higher than the  $P_{ST}$  of the second principal component score (PC2) in all valves, as it reflects most of the shape variation (Salloum et al., 2020). However, many of the raw measurements also have a high  $P_{ST}$ , similar to PC1 in some traits of the fourth and head valves, or higher than PC1 in the tail valve. Specifically, in the fourth valve, PC1 and circularity had very high  $P_{ST}$  values, indicating large phenotypic variation across populations and groups (Table 2); in the head valve, the width and perimeter are as variable as PC1, with high  $P_{ST}$  values (Table 2); and in the tail valve, height is the most phenotypically variable trait (Table 2).  $P_{ST}$  from the PC1 of the fourth valve was the most variable of the phenotypic indices. Pairwise estimates between all populations for this trait indicate the greatest phenotypic divergence between the northern and southern shape groups, but also that there is still considerable diversity

within each of these groups (Figure 3; Supplementary Table S3, Supplementary Figure S10).

### Comparison of morphological and genetic differentiation

The  $P_{ST} - F_{ST}$  comparisons detected 10 traits that are probably locally adapted at some scale, with  $P_{ST}$  and its 95% confidence interval larger than the putatively neutral  $F_{ST}$  for a critical  $cl/b^2$  ratio smaller than one (Table 2; Figure 4; Supplementary Figure S11). The majority of these comparisons (20/29 comparisons, and 9/10 traits) also had  $P_{ST}$  and its 95% confidence interval larger than  $F_{ST}$  for a critical  $cl/b^2$  ratio smaller than 0.5, indicating stronger support for local adaptation. Specifically, traits with support for local adaptation are the circularity, height, width, and PC1 of the fourth valve; the perimeter, width, and PC1 of the head valve; and the height of the tail valve (Supplementary Figure S11). Furthermore, some of these traits were consistently identified to have larger  $P_{ST}$  than  $F_{ST}$  across all three comparisons, when these indices were estimated across the 15 populations, between the North and South clades, and between the northern shape and southern shape groups (fourth valve circularity, height, width and PC1, head valve perimeter, width and PC1, tail valve height, Table 2). Three of these traits were also identified in the comparison between the Central and South clades (fourth valve circularity and PC1, tail valve height, Table 2), but none were identified in the North – Central clades comparison. It is impossible to draw firm conclusions about all the other traits and comparisons that had  $P_{ST}$  larger than  $F_{ST}$ , as either the critical  $cl/b^2$  ratio was large, or the lower 95% confidence interval of  $P_{ST}$  was smaller than  $F_{ST}$  (Supplementary Figure S11).

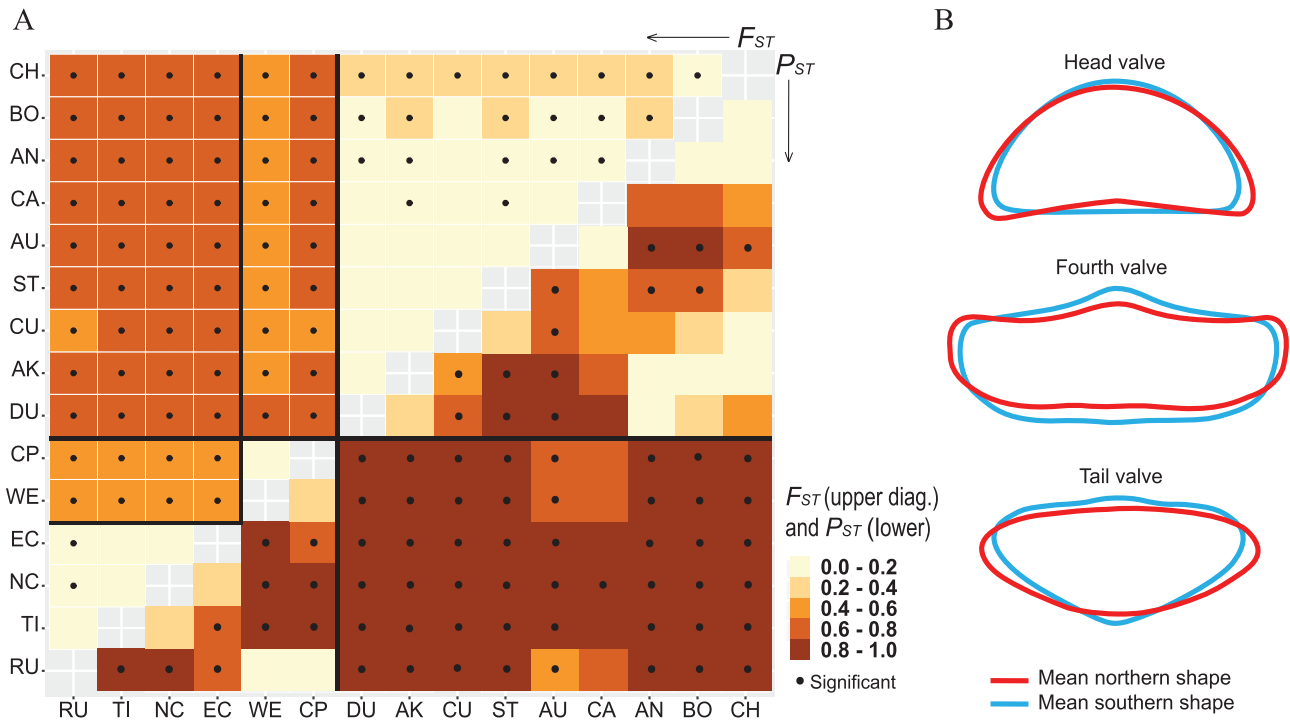


**Figure 3.** (A) Heat map of population pairwise differentiation, with darker shading corresponding to higher values. The upper diagonal corresponds to  $F_{ST}$  estimated with the putatively neutral SNPs; the lower diagonal corresponds to  $P_{ST}$  estimated for the first principal component of shape (PC1) of the fourth valve. Black dots mark results significant after correction for multiple testing in  $F_{ST}$ , and results that had a lower 95% confidence interval larger than zero in  $P_{ST}$ . Black vertical and horizontal bars separate the North, Central, and South clades in  $F_{ST}$ , and the two shape groups in  $P_{ST}$ . Population key: as per Figure 2. (B) Comparison of mean shapes found in northern versus southern groups for PC1 of the head, fourth and tail valves. Outlines were generated with SHAPE v.1.3 (Iwata & Ukai, 2002), following the methods reported in Salloum et al. (2020). SNP = single-nucleotide polymorphism.

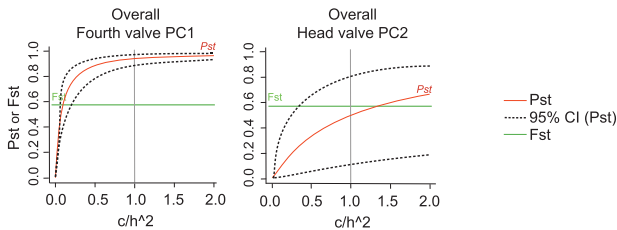


**Figure 4.** Example  $P_{ST} - F_{ST}$  comparison plots for a range of  $c/h^2$  ratios. On the left is an example of a trait (PC1 of the fourth valve) in which local adaptation is strongly supported, as the critical value of the  $c/h^2$  ratio (where  $P_{ST} = F_{ST}$ ) is  $< 0.5$ . On the right is an inconclusive case (PC2 of the fourth valve) for which  $P_{ST}$  is larger than  $F_{ST}$  only when the critical  $c/h^2$  value is  $> 1.0$ , and the 95% confidence intervals of  $P_{ST}$  are very large.  $P_{ST}$  and  $F_{ST}$  are on the y axis (range 0 to 1). The x axis corresponds to the range of  $c/h^2$  ratios used to estimate  $P_{ST}$  (from 0 to 2). 95% CI are the upper and lower 95% confidence intervals of  $P_{ST}$ . Both plots resulted from  $P_{ST}$  indices of individuals partitioned across 15 populations (overall estimates, Table 2).

In addition, none of the traits considered here are likely under stabilizing selection across populations ( $P_{ST}$  significantly smaller than  $F_{ST}$  for a critical  $c/h^2$  ratio larger than one), as the confidence intervals were very large for all traits and comparisons with low  $P_{ST}$ . Our conclusions were robust to the set of loci selected to calculate neutral  $F_{ST}$  (Supplementary Material, AMD3), as all  $P_{ST}$  values that were previously significantly higher than neutral  $F_{ST}$  (0.57) were also higher than  $F_{ST}$  calculated from all loci (0.82).

**Discussion**

Here, we have shown that in *O. neglectus* there are high levels of geographic differentiation in both genome-wide SNP

variation and phenotypic variation in shell-shape traits. The genetic differentiation reflects the low dispersal capacity of the species, given its brooding developmental mode (Creese, 1986), whereas the high phenotypic variation can be expected in species distributed over highly heterogeneous environments (Hamann et al., 2017; Volis et al., 2015). Overall, the  $P_{ST} - F_{ST}$  comparisons indicate a probable role for local adaptation, thus supporting the hypothesis that shell shape could be an adaptive trait.

The high level of population genetic differentiation and the existence of three geographically separated clades must be taken into consideration when trying to understand the relative roles of neutral and adaptive evolution on any trait. The large genetic differentiation is consistent with the brooding development in the species (Creese, 1986), and also with the differential connectivity levels within the clades, as only the South populations are frequently connected via rafting on *Durvillaea* species (Nikula et al., 2012; Salloum et al., 2020, 2022; Waters et al., 2018). Ultimately, such a strong stratification results in high  $F_{ST}$  values, which leads to conservative outcomes on the  $P_{ST} - F_{ST}$  comparisons;  $P_{ST}$  must be very high to be significantly larger than  $F_{ST}$ . Population stratification could be playing a role in the level of phenotypic differentiation observed, but there are instances in which  $P_{ST}$  values are large even when populations are genetically similar (e.g., among the South Island populations DU, AK, CU, and ST in Figure 3A), thus  $P_{ST}$  results are unlikely to have been strongly influenced by population subdivision.

We focused on the genetic variation that is presumed to be selectively neutral, so as to compare directly with the observed phenotypic variation by using  $P_{ST} - F_{ST}$  comparisons. Since *O. neglectus* population structure is strong (Salloum et al.,

2022, see also  $F_{ST}$  distribution in [Supplementary Figure S12](#)), non-adaptive, but differentially fixed loci among clades could have been detected as outliers and removed from the dataset, lowering the neutral  $F_{ST}$ . However, this is unlikely to impact our conclusions, as our results are robust to calculating  $F_{ST}$  from all loci. Furthermore, it is possible when calculating  $P_{ST}$  to generate values close to 1 if the (sampled) within-population variance is very close to zero. However, the variance within groups was never zero, indicating that our  $P_{ST}$  calculations are statistically robust ([Supplementary Tables S4–S8](#)). Finally, due to the strong population structure, some slight increase in sampling variance could be expected in the  $P_{ST}$  values, given previously studied statistical properties of  $Q_{ST}$  ([Miller et al., 2008](#)). However, the small magnitude of the excess in sampling variance is unlikely to change conclusions for shell traits in which  $P_{ST}$  is much higher than  $F_{ST}$ .

Previous analyses indicated a much more significant gene flow within the South clade than within the other two clades, and lack of current gene flow among clades, as well as a negative correlation of migration rates with geographical distance ([Salloum et al., 2022](#)). The high  $F_{ST}$  among clades reported here, in combination with the available knowledge on population structure and demography, could lead to consideration of the three *O. neglectus* clade as different species. If this were the case, the approach undertaken here would have reduced relevance. However, this subdivision into different species is not supported by the morphological patterns, which aggregate two of the highly divergent genetic clades into one single shell shape (North + Central). As reported elsewhere, genetic data or morphology in isolation seem insufficient for species determination in brooding chitons ([Sigwart & Chen, 2017](#)), and the challenges of using external shell morphology for taxonomy in chitons are well known ([Ibáñez et al., 2020](#); [Sigwart et al., 2013](#); [Sirenko, 2006](#)). Thus, even though *O. neglectus* genetic divergence among clades is substantial, determining the species status of each individual clade is beyond the scope of this study.

The phenotypic differentiation in shell traits across populations is very variable, with a range of  $P_{ST}$  values for the different traits analyzed, which did not show correlation with geographical distance among populations. The highest  $P_{ST}$  values generally result from the estimates over all populations and comparisons of the South clade with either the North or the Central clades, indicating that the phenotypic differentiation across populations is mostly driven by the major northern versus southern shell shape differences detected previously ([Salloum et al., 2020](#)).

Considering the high level of neutral genetic divergence between the three clades, and the high  $F_{ST}$  estimates, it is surprising to find most traits with  $P_{ST}$  above  $F_{ST}$ . The robustness of  $P_{ST}$  as a  $Q_{ST}$  proxy depends on the critical value of the  $clh^2$  ratio ([Brommer, 2011](#)): a moderately small critical  $clh^2$  value between 0.5 and 1.0 makes it impossible to either fully reject the neutral expectation or to fully disregard local adaptation, as the significance of the  $P_{ST} - F_{ST}$  difference is not very robust in this less conservative scenario ([Brommer, 2011](#)). The  $P_{ST}$  estimates for many of the traits included here fall within this less conservative framework and may reflect at least some phenotypic differentiation related to non-genetic effects ([Brommer, 2011](#); [Leinonen et al., 2013](#); [Merilä, 1997](#)). However, nine of the shell traits (capturing 20 comparisons at different geographic scales) show robust differences between  $P_{ST}$  and  $F_{ST}$  with a critical  $clh^2$  value smaller than 0.5, strongly

supporting local adaptation as a mechanism increasing phenotypic differentiation among populations ([Brommer, 2011](#)), and suggesting an adaptive role for shell shape. To the best of our knowledge, this is the first evaluation of phenotypic variation using such comprehensive measurements on the exterior of chiton shells, and it is interesting to note that the first principal component scores of the fourth and head valves, as well as some of the raw traits (circularity and height of the fourth valve, width of the head valve, and height of the tail valve) had  $P_{ST}$  consistently larger than  $F_{ST}$  for very small critical  $clh^2$  ratios ( $<< 0.5$ ) in all geographical scales (except North vs. Central clades). Due to the limited information on the function of the overall external shape of chiton valves, it is challenging to further explain the specific meaning of these findings for the animal, but these traits could be either performing an adaptive role in the shape of *O. neglectus* valves, or be correlated with other traits that are adaptive (the first principal component in particular is likely to aggregate most of the adaptive signal from the raw traits it is based on). Furthermore, if all six intermediate valves in chitons are assumed to be similar in shape and function, it is possible that all intermediate valves of *O. neglectus* are under the same type of selection acting on the fourth valve. It is important to note, however, that traits of the same valve are not completely independent. Overall, the significant traits observed here describe broad differences in chiton shell shape that support a scenario of local adaptation. However, due to the nature of  $P_{ST} - F_{ST}$  comparisons, phenotypic plasticity could also be inflating  $P_{ST}$  values and cannot be completely disregarded ([Brommer et al., 2014](#); [Seymour et al., 2019](#)).

An adaptive role for shell shape has been observed in other mollusc species ([Johannesson, 1986](#); [Kess & Boulding, 2019](#); [Newkirk & Doyle, 1975](#); [Van Bocxlaer et al., 2020](#)), but even though there are studies focusing on the biomechanics of chiton shells ([Connors et al., 2012](#); [Sigwart et al., 2015](#)), and on biomineralization ([Varney et al., 2021](#)), to our knowledge, this is the first time in which potentially adaptive diversity is assessed and reported for external chiton shell shape traits. Environmental variation seems to be important for diversification in chiton shell shape ([Sirenko, 2006](#)), and functional variation in chiton shell morphology has been hypothesized to be linked to factors such as wave exposure and local topology ([Horn, 1983](#); [Sigwart et al., 2015](#)). Here, the  $P_{ST} - F_{ST}$  comparisons indicate a probable role for local adaptation, thus supporting the hypothesis that *O. neglectus* shell shape variation could be adaptive, potentially correlated with the ability to live and raft in the holdfast of *Durvillaea* species ([Salloum et al., 2020](#)). The outline of the shape of each of the three valves generated with the previous geometric morphometric analyses ([Salloum et al., 2020](#)) suggests that populations of the South clade appear to have an overall narrower and more elongated shell, which may assist in their use of holdfast crevices in these environments ([Figure 3B](#), [Supplementary Figure S10](#)). The selective pressure in this case could be due to differences in crevice shape and size, or the water flow experienced by *O. neglectus* in a holdfast, versus that found under boulders. In addition, differences in predation pressure and sexual selection have been linked to differences in molluscs shell shape before ([Estévez et al., 2020](#); [Johannesson, 1986](#); [Kess & Boulding, 2019](#); [Schilthuizen et al., 2007a, 2007b](#)). However, even in the well-studied field of stream ecology and invertebrate adaptation to water flow, it is challenging to determine the specific selective pressures driving shell shape

adaptive differentiation (Statzner, 2008; Verhaegen et al., 2019). Finally, factors other than those of the specific niche could be posing selective pressures on these highly divergent clades and relatively isolated populations. *O. neglectus* is distributed over a latitudinal environmental gradient, and for a species with such a strong population stratification, there could be strong environmental differentiation, driving local adaptation to various factors. This study concentrated on the neutral genetic variation observed in this species, to compare directly with the morphological variation observed. Further research on chiton shell adaptive variation, and how this correlates with environmental differences, can lead to deeper understanding not only of factors driving chiton shell diversification, but of molluscs' shell evolution as a whole.

## Supplementary material

Supplementary material is available online at *Evolution* (<https://academic.oup.com/evolut/qpac011>)

## Data availability

The data and the scripts for analyses used in this manuscript are available from Figshare, with the following DOIs:

$P_{ST}$ - $F_{ST}$  comparisons: <https://doi.org/10.5061/dryad.xd2547dm5>;

Morphological data: <https://doi.org/10.17608/k6.auckland.12291200.v1> (Salloum et al., 2020);

Raw sequence files: <https://doi.org/10.17608/k6.auckland.19388579.v1> (Salloum et al., 2022);

De-multiplexed sequence files (fastq): <https://doi.org/10.17608/k6.auckland.19365608>

## Author contributions

All authors conceived the study. P.M.S. performed the experiments and data analyses. All authors contributed to drafting and revising the manuscript, and gave final approval for this version to be submitted for consideration for publication.

## Funding statement

This research was supported by the New Zealand Department of Conservation and a graduate student research fund from the Society of Systematic Biologists. P.M.S. was supported by a University of Auckland Doctoral Scholarship.

*Conflict of interest:* The authors declare no conflict of interest.

## Acknowledgments

We thank Prof. Hamish Spencer, Prof Jon Waters, Dr Ceridwen Fraser, Dr Raisa Nikula, and Dr Tania King for making their samples from the South Island and remote Sub-Antarctic Islands available. We also thank Prof. Mary Morgan-Richards for her intellectual advice. We thank Dr Vibha Thakur for help in the wet laboratory, and all field assistants (Airton C. Agostinho, Dr. Bryce Peebles, Sarah Brand, and Dr Dyahruri Sanjayasarit) for all the effort put into searching and collecting chitons.

## References

Ab-Ghani, N. I., Herczeg, G., and Merila, J. (2012). Body size divergence in nine-spined sticklebacks: Disentangling additive genetic and

- maternal effects. *Biological Journal of the Linnean Society*, 107(3), 521–528. <https://doi.org/10.1111/j.1095-8312.2012.01956.x>
- Alexander, A. (2018). GBS\_SNP\_filter v1.x.x. GitHub repository. [https://github.com/laninsky/GBS\\_SNP\\_filter](https://github.com/laninsky/GBS_SNP_filter)
- Benjamini, Y., & Yekutieli, D. (2001). The control of the false discovery rate in multiple testing under dependency. *Annals of Statistics*, 29(4), 1165–1188. <https://doi.org/10.1214/aos/1013699998>
- Blanquart, F., Kaltz, O., Nuismer, S. L., & Gandon, S. (2013). A practical guide to measuring local adaptation. *Ecology Letters*, 16(9), 1195–1205. <https://doi.org/10.1111/ele.12150>
- Brommer, J. E. (2011). Whither Pst? The approximation of Qst by Pst in evolutionary and conservation biology. *Journal of Evolutionary Biology*, 24(6), 1160–1168. <https://doi.org/10.1111/j.1420-9101.2011.02268.x>
- Brommer, J. E., Hanski, I. K., Kekkonen, J., & Väisänen, R. A. (2014). Size differentiation in Finnish house sparrows follows Bergmann's rule with evidence of local adaptation. *Journal of Evolutionary Biology*, 27(4), 737–747. <https://doi.org/10.1111/jeb.12342>
- Catchen, J. M., Amores, A., Hohenlohe, P., Cresko, W., & Postlethwait, J. H. (2011). Stacks: Building and genotyping Loci de novo from short-read sequences. *G3*, 1(3), 171–182. <https://doi.org/10.1534/g3.111.000240>
- Catchen, J., Hohenlohe, P. A., Bassham, S., Amores, A., & Cresko, W. A. (2013). Stacks: An analysis tool set for population genomics. *Molecular Ecology*, 22(11), 3124–3140. <https://doi.org/10.1111/mec.12354>
- Connors, M. J., Ehrlich, H., Hog, M., Godefroy, C., Araya, S., Kallai, I., Gazit, D., Boyce, M., & Ortiz, C. (2012). Three-dimensional structure of the shell plate assembly of the chiton *Tonicella marmorea* and its biomechanical consequences. *Journal of Structural Biology*, 177(2), 314–328. <https://doi.org/10.1016/j.jsb.2011.12.019>
- Creese, R. G. (1986). Brooding behaviour and larval development in the New Zealand chiton, *Onithochiton neglectus* de Rochebrune (Mollusca: Polyplacophora). *New Zealand Journal of Zoology*, 13(1), 83–91. <https://doi.org/10.1080/03014223.1986.10422648>
- Creese, R. G. (1988). Ecology of molluscan grazers and their interactions with marine algae in north-eastern New Zealand: A review. *New Zealand Journal of Marine and Freshwater Research*, 22(3), 427–444. <https://doi.org/10.1080/00288330.1988.9516314>
- Danecek, P., Auton, A., Abecasis, G., Albers, C. A., Banks, E., DePristo, M. A., Handsaker, R. E., Lunter, G., Marth, G. T., Sherry, S. T., McVean, G., & Durbin, R.; 1000 Genomes Project Analysis Group. (2011). The variant call format and VCFtools. *Bioinformatics*, 27(15), 2156–2158. <https://doi.org/10.1093/bioinformatics/btr330>
- de Villemereuil, P., Gaggiotti, O., & Goudet, J. (2020). Common garden experiments to study local adaptation need to account for population structure. *Journal of Ecology*, 110, 1005–1009. <https://doi.org/10.1111/1365-2745.13528>
- de Villemereuil, P., Gaggiotti, O. E., Mouterde, M., & Till-Bottraud, I. (2016). Common garden experiments in the genomic era: New perspectives and opportunities. *Heredity*, 116(3), 249–254. <https://doi.org/10.1038/hdy.2015.93>
- Dray, S. and Dufour, A.-B. (2007). The ade4 Package: Implementing the duality diagram for ecologists. *Journal of Statistical Software*, 22(4), 1–20. <https://doi.org/10.18637/jss.v022.i04>
- Estévez, D., Kozminsky, E., Carvajal-Rodríguez, A., Caballero, A., Faria, R., Galindo, J., and Rolán-Alvarez, E. (2020). Mate choice contributes to the maintenance of shell color polymorphism in a marine snail via frequency-dependent sexual selection. *Frontiers in Marine Science*, 7, 614237. <https://doi.org/10.3389/fmars.2020.614237>
- Foll, M., & Gaggiotti, O. (2008). A genome-scan method to identify selected loci appropriate for both dominant and codominant markers: A Bayesian perspective. *Genetics*, 180(2), 977–993. <https://doi.org/10.1534/genetics.108.092221>
- Frichot, E., & François, O. (2015). LEA: An R package for landscape and ecological association studies. *Methods in Ecology and Evolution*, 6, 925–929. <https://doi.org/10.1111/2041-210X.12382>
- Grenier, S., Barre, P., & Litrico, I. (2016). Phenotypic plasticity and selection: Nonexclusive mechanisms of adaptation. *Scientifica*, 2016, 7021701. <https://doi.org/10.1155/2016/7021701>

- Hamann, E., Scheepens, J. F., Kesselring, H., Armbruster, G. F. J., & Stöcklin, J. (2017). High intraspecific phenotypic variation, but little evidence for local adaptation in *Geum reptans* populations in the Central Swiss Alps. *Alpine Botany*, 127(2), 121–132. <https://doi.org/10.1007/s00035-017-0185-y>
- Horn, P. L. (1983). *Energetics of the chiton Sypharochiton pelliserpentis from a sheltered shore at Kaikoura*. Zoology. MSc thesis. University of Canterbury, Christchurch, New Zealand. <http://dx.doi.org/10.26021/5735>
- Ibáñez, C. M., Pardo-Gandarillas, M. C., Méndez, M. A., Sellanes, J., Sigwart, J. D., & Sirenko, B. (2020). Phylogenetic position and morphological descriptions of Chiton species from the south-eastern Pacific. *Zoological Journal of the Linnean Society*, 10(3), 1–25. <https://doi.org/10.1093/zoolinnean/zlaa067>
- Iwata, H., & Ukai, Y. (2002). SHAPE: A computer program package for quantitative evaluation of biological shapes based on elliptic Fourier descriptors. *The Journal of Heredity*, 93, 384–385.
- Johannesson, B. (1986). Shell morphology of *Littorina saxatilis* Oliv.: The relative importance of physical factors and predation. *Journal of Experimental Marine Biology and Ecology*, 102(2–3), 183–195.
- Jombart, T. (2008). adegenet: A R package for the multivariate analysis of genetic markers. *Bioinformatics*, 24(11), 1403–1405. <https://doi.org/10.1093/bioinformatics/btn129>
- Jombart, T., & Ahmed, I. (2011). adegenet 1.3-1: New tools for the analysis of genome-wide SNP data. *Bioinformatics*, 27(21), 3070–3071. <https://doi.org/10.1093/bioinformatics/btr521>
- Kamvar, Z. N., Brooks, J. C., & Grünwald, N. J. (2015). Novel R tools for analysis of genome-wide population genetic data with emphasis on clonality. *Frontiers in Genetics*, 6, 1–10. <https://doi.org/10.3389/fgene.2015.00208>
- Kamvar, Z. N., Tabima, J. F., & Grünwald, N. J. (2014). Poppr: An R package for genetic analysis of populations with clonal, partially clonal, and/or sexual reproduction. *PeerJ*, 2, e281. <https://doi.org/10.7717/peerj.281>
- Kawecki, T. J., & Ebert, D. (2004). Conceptual issues in local adaptation. *Ecology Letters*, 7(12), 1225–1241. <https://doi.org/10.1111/j.1461-0248.2004.00684.x>
- Kess, T., & Boulding, E. G. (2019). Genome-wide association analyses reveal polygenic genomic architecture underlying divergent shell morphology in Spanish *Littorina saxatilis* ecotypes. *Ecology and Evolution*, 9(17), 1–15. <https://doi.org/10.1002/ece3.5378>
- Leinonen, T., McCairns, R. J., O'Hara, R. B., & Merilä, J. (2013). Q(ST)-F(ST) comparisons: Evolutionary and ecological insights from genomic heterogeneity. *Nature Reviews. Genetics*, 14(3), 179–190. <https://doi.org/10.1038/nrg3395>
- Meirmans, P. G., & Hedrick, P. W. (2011). Assessing population structure: F(ST) and related measures. *Molecular Ecology Resources*, 11(1), 5–18. <https://doi.org/10.1111/j.1755-0998.2010.02927.x>
- Merilä, J. (1997). Quantitative trait and allozyme divergence in the Greenfinch (*Carduelis chloris*, Aves: Fringillidae). *Biological Journal of the Linnean Society*, 61(2), 243–266. <https://doi.org/10.1006/bjil.1996.0120>
- Merilä, J., & Crnokrak, P. (2001). Comparison of genetic differentiation at marker loci and quantitative traits. *Journal of Evolutionary Biology*, 14(6), 892–903. <https://doi.org/10.1046/j.1420-9101.2001.00348.x>
- Miller, J. R., Wood, B. P., & Hamilton, M. B. (2008). F(ST) and Q(ST) under neutrality. *Genetics*, 180(2), 1023–1037. <https://doi.org/10.1534/genetics.108.092031>
- Morton, J., & Miller, M. (1973). *The New Zealand sea shore*. Collins.
- Naylor, M. (1951). The New Zealand species of *Durvillea*. *The Transactions and Proceedings of the Royal Society of New Zealand*, 80(4), 277–297.
- Newkirk, G. F., & Doyle, R. W. (1975). Genetic analysis of shell-shape variation in *Littorina saxatilis* on an environmental cline. *Marine Biology*, 30, 227–237. <https://doi.org/10.1007/BF00390745>
- Nikula, R., Spencer, H. G., & Waters, J. M. (2012). Passive rafting is a powerful driver of transoceanic gene flow. *Biology Letters*, 9(1), 20120821. <https://doi.org/10.1098/rsbl.2012.0821>
- Outomuro, D., & Johansson, F. (2017). A potential pitfall in studies of biological shape: Does size matter? *The Journal of Animal Ecology*, 86(6), 1447–1457. <https://doi.org/10.1111/1365-2656.12732>
- Paradis, E. (2010). pegas: An R package for population genetics with an integrated-modular approach. *Bioinformatics*, 26(3), 419–420. <https://doi.org/10.1093/bioinformatics/btp696>
- Peakall, R., & Smouse, P. E. (2006). GENALEX 6: Genetic analysis in Excel. Population genetic software for teaching and research. *Molecular Ecology Resources*, 6(1), 288–295. <https://doi.org/10.1111/j.1471-8286.2005.01155.x>
- Peakall, R., & Smouse, P. E. (2012). GenALEX 6.5: Genetic analysis in Excel. Population genetic software for teaching and research—an update. *Bioinformatics*, 28(19), 2537–2539. <https://doi.org/10.1093/bioinformatics/bts460>
- Pujol, B., Wilson, A. J., Ross, R. I., & Pannell, J. R. (2008). Are Q(ST)-F(ST) comparisons for natural populations meaningful? *Molecular Ecology*, 17(22), 4782–4785. <https://doi.org/10.1111/j.1365-294X.2008.03958.x>
- Salloum, P. M., De Villemereuil, P., Santure, A. W., Waters, J. M., & Lavery, S. D. (2020). Hitchhiking consequences for genetic and morphological patterns: The influence of kelp-rafting on a brooding chiton. *Biological Journal of the Linnean Society*, 130(4), 756–777. <https://doi.org/10.1093/biolinnean/blaa073>
- Salloum, P. M., Santure, A. W., Lavery, S. D., & de Villemereuil, P. (2022). Finding the adaptive needles in a population-structured haystack: A case study in a New Zealand mollusc. *Journal of Animal Ecology*, 91(6), 1–13. <https://doi.org/10.1111/1365-2656.13692>
- Sanford, E., & Kelly, M. W. (2011). Local adaptation in marine invertebrates. *Annual Review of Marine Science*, 3, 509–535. <https://doi.org/10.1146/annurev-marine-120709-142756>
- Santure, A. W., & Wang, J. (2009). The joint effects of selection and dominance on the QST - FST contrast. *Genetics*, 181(1), 259–276. <https://doi.org/10.1534/genetics.108.097998>
- Schilthuizen, M., Craze, P. G., Cabanban, A. S., Davison, A., Stone, J., Gittenberger, E., & Scott, B. J. (2007a). Sexual selection maintains whole-body chiral dimorphism in snails. *Journal of Evolutionary Biology*, 20(5), 1941–1949. <https://doi.org/10.1111/j.1420-9101.2007.01370.x>
- Schilthuizen, M., van Til, A., Salverda, M., Liew, T. S., James, S. S., bin Elahan, B., & Vermeulen, J. J. (2007b). Microgeographic evolution of snail shell shape and predator behavior. *Evolution*, 60(9), 1851–1858. <https://doi.org/10.1554/06-114.1>
- Seymour, M., Rasanen, K., & Kristjansson, B. K. (2019). Drift versus selection as drivers of phenotypic divergence at small spatial scales: The case of Belgjarskogur threespine stickleback. *Ecology and Evolution*, 9(14), 8133–8145. <https://doi.org/10.1002/ece3.5381>
- Sigwart, J. D. (2009). Morphological cladistic analysis as a model for character evaluation in primitive living chitons (Polyplacophora, Lepidopleurina). *American Malacological Bulletin*, 27(1/2), 95–104. <https://doi.org/10.4003/006.027.0208>
- Sigwart, J. D., & Chen, C. (2017). Life history, patchy distribution, and patchy taxonomy in a shallow-water invertebrate (Mollusca: Polyplacophora: Lepidopleurida). *Marine Biodiversity*, 48, 1867–1877. <https://doi.org/10.1007/s12526-017-0688-1>
- Sigwart, J. D., Green, P. A., & Crofts, S. B. (2015). Functional morphology in chitons (Mollusca, Polyplacophora): Influences of environment and ocean acidification. *Marine Biology*, 162(11), 2257–2264. <https://doi.org/10.1007/s00227-015-2761-2>
- Sigwart, J. D., & Lindberg, D. R. (2015). Consensus and confusion in molluscan trees: Evaluating morphological and molecular phylogenies. *Systematic Biology*, 64(3), 384–395. <https://doi.org/10.1093/sysbio/syu105>
- Sigwart, J. D., Stoeger, I., Kneibelsberger, T., & Schwabe, E. (2013). Chiton phylogeny (Mollusca: Polyplacophora) and the placement of the enigmatic species *Chorioplax grayi* (H. Adams & Angas). *Invertebrate Systematics*, 27(6), 603–621. <https://doi.org/10.1071/IS13013>
- Silva, S. B., & Silva, A. (2018). Pstat: An R package to assess population differentiation in phenotypic traits. *The R Journal*, 10(1), 447–454. <https://doi.org/10.32614/rj-2018-010>

- Sirenko, B. (2006). New outlook on the system of chitons (Mollusca: Polyplacophora). *Venus*, 65(1-2), 27–49.
- Spalding, M. D., Agostini, V. N., Rice, J., & Grant, S. M. (2012). Pelagic provinces of the world: A biogeographic classification of the world's surface pelagic waters. *Ocean & Coastal Management*, 60, 19–30. <https://doi.org/10.1016/j.ocecoaman.2011.12.016>
- Spitze, K. (1993). Population structure in *Daphnia obtusa*: Quantitative genetic and allozymic variation. *Genetics*, 135(2), 367–374. <https://doi.org/10.1093/genetics/135.2.367>
- Statzner, B. (2008). How views about flow adaptations of benthic stream invertebrates changed over the last century. *International Review of Hydrobiology*, 93(4-5), 593–605. <https://doi.org/10.1002/iroh.200711018>
- Van Bocxlaer, B., Ortiz-Sepulveda, C. M., Gurdebeke, P. R., & Veke-mans, X. (2020). Adaptive divergence in shell morphology in an ongoing gastropod radiation from Lake Malawi. *BMC Evolutionary Biology*, 20(1), 5. <https://doi.org/10.1186/s12862-019-1570-5>
- Varney, R. M., Speiser, D. I., McDougall, C., Degnan, B. M., & Kocot, K. M. (2021). The iron-responsive genome of the Chiton *Acantho-pleura granulata*. *GBE*, 13(1), evaa263. <https://doi.org/10.1093/gbe/evaa263>
- Verhaegen, G., Herzog, H., Korsch, K., Kerth, G., Brede, M., & Haase, M. (2019). Testing the adaptive value of gastropod shell morphology to flow: A multidisciplinary approach based on morphometrics, computational fluid dynamics and a flow tank experiment. *Zoological Letters*, 5, 5. <https://doi.org/10.1186/s40851-018-0119-6>
- Volis, S., Ormanbekova, D., Yermekbayev, K., Song, M., & Shulgina, I. (2015). Multi-approaches analysis reveals local adaptation in the emmer wheat (*Triticum dicoccoides*) at macro- but not micro-geographical scale. *PLoS ONE*, 10(3), e0121153. <https://doi.org/10.1371/journal.pone.0121153>
- Waters, J. M., King, T. M., Fraser, C. I., & Craw, D. (2018). An integrated ecological, genetic and geological assessment of long-distance dispersal by invertebrates on kelp rafts. *Frontiers of Biogeography*, 10(3-4), 1–13. <https://doi.org/10.21425/F5FBG40888>
- Whitlock, M. C., & Gilbert, K. J. (2012). Q(ST) in a hierarchically structured population. *Molecular Ecology Resources*, 12(3), 481–483. <https://doi.org/10.1111/j.1755-0998.2012.03122.x>